Synthesis, spectroscopic characterization and in vitro antimicrobial activity of diorganotin(IV) dichloride adducts with [1,2,4]triazolo-[1,5-*a*]pyrimidine and 5,7-dimethyl-[1,2,4]triazolo-[1,5-*a*]pyrimidine

M. Assunta Girasolo [a], Domenico Schillaci [b], Clelia Di Salvo [a], Giampaolo Barone [a], Arturo Silvestri [a], Giuseppe Ruisi [a,*]

[a] *Dipartimento di Chimica Inorganica e Analitica Stanislao Cannizzaro, Università di Palermo, Viale delle Scienze, Edificio 17, I-90128 Palermo, Italy*
[b] *Dipartimento di Chimica e Tecnologia Farmaceutiche, Università di Palermo, via Archirafi 32, I-90123 Palermo, Italy*

Abstract

The heterocyclic ligands [1,2,4]triazolo-[1,5-*a*]pyrimidine (tp) and 5,7-dimethyl-[1,2,4]triazolo-[1,5-*a*]pyrimidine (dmtp), react with diorganotin dichlorides giving the addition compounds $Me_2SnCl_2(tp)_2$, $Et_2SnCl_2(tp)_2$, $Me_2SnCl_2(dmtp)_2$, $Et_2SnCl_2(dmtp)_2$, $Bu_2SnCl_2(dmtp)$, $Ph_2SnCl_2(dmtp)$. The organotin:ligand stoichiometry goes from 1:2 to 1:1 by increasing the steric hindrance of the organic groups bound to tin. The compounds have been characterized by means of infrared, ^{119}Sn Mössbauer and ^1H AND ^{13}C NMR spectroscopy.

The ligands presumably coordinate to tin classically through the nitrogen atom at the position 3. The 1:1 complexes adopt trigonal bipyramidal structures, with the organic groups on the equatorial plane and the ligand in the apical position. All-*trans* octahedral structures are inferred for the 1:2 complexes, except for $Et_2SnCl_2(tp)_2$, characterized by a skew-trapezoidal structure.

^{119}Sn Mössbauer measurements, at room temperature, in concomitance with DFT calculations, performed on isomeric structures of $R_2SnCl_2(tp)_2$ (R = Me, Et), allowed us to conclude that the all-trans octahedral coordination induces self-assembly in the solid state, possibly accomplished through π–π stacking interactions among the planar ligands coordinated to the organotin(IV) compound, while the skew-trapezoidal structure attributed to $Et_2SnCl_2(tp)_2$, induces the formation of monomeric adducts in the solid state.

In vitro antimicrobial tests showed that [*n*-$Bu_2SnCl_2(dmtp)$] has interesting properties as anti Gram-positive and antibiofilm agent.
© 2005 Elsevier B.V. All rights reserved.

Keywords: Triazolopyrimidine; Diorganotin(IV); Mössbauer; DFT calculations; Antimicrobial activity

1. Introduction

The interaction of metal ions with [1,2,4]-triazolo[1,5-*a*]pyrimidine derivatives has been widely investigated [1,2], the interest mainly arising from their biological properties and from the circumstance that triazolopyrimidine ring has a chemical structure similar to purine, from which it differs for the presence of a pyrimidine nitrogen atom in a bridgehead position and the consequent disappearance of the acidic hydrogen atom of the five-membered ring [1]. We have recently reported on the synthesis, characterization and antimicrobial activity of organotin(IV) derivatives of oxo-substituted triazolopyrimidines [3]. Polymeric compounds were obtained, where exocyclic oxygen atoms are involved in the coordination. [1,2,4]triazolo-[1,5-*a*]pyrimidine (tp) and its derivative 5,7-dimethyl-[1,2,4]triazolo-[1,5-*a*]pyrimidine (dmtp) (see Fig. 1) may also give polymeric compounds through N(1), N(3) coordination [1], but they
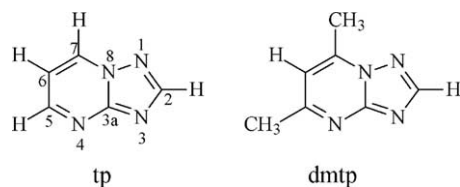

Fig. 1. The ligands employed and the atom numbering scheme.

normally act as monodentate ligands, the preferred binding position being N(3) [1]. A few compounds have also been described, in which there is not a direct bond between the metal atom and the triazolopyrimidine derivative. Among these, the tin(IV) compound $[H_2dmtp]_2[SnCl_6]$ [4], where the $[Hdmtp]^+$ cation is protonated at N(3). Continuing our research in the field, we report here the results of infrared, ^{119}Sn Mössbauer, ^1H and ^{13}C NMR spectroscopic studies on diorganotin(IV) dichloride adducts of tp and dmtp, see Fig. 1, and of antimicrobial activity tests on both fungi (*Candida albicans*, *Candida tropicalis*) and bacteria (*Escherichia coli*, *Pseudomonas aeruginosa*, *Staphylococcus aureus*).

2. Experimental

2.1. Materials and methods

The products employed in the present study were purchased from C. Erba (Milan, Italy), Sigma–Aldrich (Milan, Italy), and Merck KGaA (Germany), and used without further purification except methanol, which was distilled over magnesium.

Carbon, hydrogen and nitrogen assays were carried out with a Vario EL III elemental analyzer (Elementar GmbH, Germany); chlorine was determined by potentiometric titration with standard silver nitrate after combustion in pure oxygen according to Schöniger [5].

Infrared spectra (nujol and hexachlorobutadiene mulls, CsI windows) were recorded with an FT-IR spectrometer Perkin–Elmer Spectrum One. Selected bands are reported in Table 1.

The Mössbauer (nuclear γ resonance) spectrometers, the related instrumentation and data reduction procedures were as previously described [6]. A 10-mCi Ca $^{119}SnO_3$ source (RITVERC GmbH, St. Petersburg, Russia) was employed. The isomer shifts (δ) are relative to room temperature Ca$^{119}SnO_3$. Methanol solution spectra were recorded on 0.1 M samples, frozen by immersion in liquid nitrogen. The ^{119}Sn Mössbauer parameters are reported in Table 2.

^1H and ^{13}C NMR spectra in deuterated methanol, reported in Tables 4 and 5, were recorded with a Bruker AC 250 E instrument operating at 250 and 63 MHz respectively.

2.2. Synthesis of the adducts

The adducts were obtained by reacting the diorganotin(IV) dichlorides with the ligands as detailed below.

Dimethyl- and diethyltin derivatives: the organotin dichloride (2 mmol) and the ligand (4 mmol) were mixed in diethyl ether (20 mL). The ligand is sparingly soluble in such conditions. The suspension was stirred at room temperature for 24 h, then the residue collected and dried under vacuum.

$[Me_2SnCl_2(tp)_2]$ (**1**) m.p. 140–142 °C. Anal. Calc. for $C_{12}H_{14}Cl_2N_8Sn$ (459.91 g mol^{-1}): C, 31.34; H, 3.07; N, 24.36; Cl, 15.42. Found: C, 31.32; H, 2.94; N, 24.02; Cl, 15.49%.

$[Et_2SnCl_2(tp)_2]$ (**2**) m.p. 108–110 °C. Anal. Calc. for $C_{14}H_{18}Cl_2N_8Sn$ (487.97 g mol^{-1}): C, 34.46; H, 3.72; N, 22.96; Cl, 14.53. Found: C, 34.34; H, 3.28; N, 22.96; Cl, 14.79%.

Table 1
Selected IR bands (cm^{-1}) for diorganotin(IV) chloride adducts

	Compound	ν_{tp}	ν_{py}	ν(Sn–Cl)	ν(Sn–C)
	tp	1621m	1533m		
			1515m		
1	Me$_2$SnCl$_2$(tp)$_2$[a]	1616vs	1539s	255s	
			1521s		
			1508s		
2	Et$_2$SnCl$_2$(tp)$_2$	1619vs	1540m	322s	533w(asym)
			1520s	251s	497w(sym)
	dmtp	1637s	1547vs		
3	Me$_2$SnCl$_2$(dmtp)$_2$	1632s	1549s	259s	573mw
		1618m			
4	Et$_2$SnCl$_2$(dmtp)$_2$	1632m	1552vs	231m	
		1622s			
5	n-Bu$_2$SnCl$_2$(dmtp)	1634s	1550vs	329s	
		1621s		270s	
6	Ph$_2$SnCl$_2$(dmtp)[b]	1635m	1550s	287m	
		1622m		267s	

Abbreviations: vs, very strong; s, strong; m, medium; w, weak.
[a] 796s = ρ(CH$_3$).
[b] 1431s = ν(C=C); 997mw = ring vibration; 731vs, 695s = C–H out of plane [30].

Table 2
^{119}Sn Mössbauer parameters of diorganotin(IV) chlorides and their tp and dmtp adducts[a]

Compound		δ[b] (mm s^{-1})	ΔE[c] (mm s^{-1})	Γ[d] (mm s^{-1})	Area (mm s^{-1})
1	Me$_2$SnCl$_2$(tp)$_2$	1.41	4.16	0.86	0.0780
	at 294 K	1.38	4.11	0.84	0.0075
	MeOH sol., 0.1 M	1.38	4.10	0.82	
2	Et$_2$SnCl$_2$(tp)$_2$	1.51	3.45	0.80	
	MeOH sol., 0.1 M	1.56	4.02	0.82	
3	Me$_2$SnCl$_2$(dmtp)$_2$	1.44	4.00	0.81	
	MeOH sol., 0.1 M	1.41	3.91	0.82	
4	Et$_2$SnCl$_2$(dmtp)$_2$	1.59	4.02	0.77	
	MeOH sol., 0.1 M	1.55	3.91	0.79	
5	n-Bu$_2$SnCl$_2$(dmtp)	1.45	3.24	0.79	
	MeOH sol., 0.1 M	1.54	4.01	0.84	
6	Ph$_2$SnCl$_2$(dmtp)	1.26	2.89	0.84	
	MeOH sol., 0.1 M	1.28	3.65	0.84	
	Me$_2$SnCl$_2$, MeOH sol., 0.1 M	1.41	3.92	0.82	
	Et$_2$SnCl$_2$, MeOH sol., 0.1 M	1.55	4.07	0.85	
	n-Bu$_2$SnCl$_2$, MeOH sol., 0.1 M	1.55	3.90	0.87	
	Ph$_2$SnCl$_2$, MeOH sol., 0.1 M	1.32	3.67	0.93	

[a] In the solid state and at liquid-nitrogen temperature, unless otherwise specified.
[b] Isomer shift with respect to room-temperature CaSnO$_3$.
[c] Nuclear quadrupole splitting.
[d] Full width at half-height of the resonant peaks.

[Me$_2$SnCl$_2$(dmtp)$_2$] (**3**) m.p. 94–96 °C. Anal. Calc. for C$_{16}$H$_{22}$Cl$_2$N$_8$Sn (516.02 g mol^{-1}): C, 37.24; H, 4.30; N, 21.72; Cl, 13.74. Found: C, 37.20; H, 4.00; N, 21.54; Cl, 13.76%.

[Et$_2$SnCl$_2$(dmtp)$_2$] (**4**) m.p. 85–87 °C. Anal. Calc. for C$_{18}$H$_{26}$Cl$_2$N$_8$Sn (544.08 g mol^{-1}): C, 39.74; H, 4.82; N, 20.60; Cl, 13.03. Found: C, 39.90; H, 4.50; N, 20.90; Cl, 13.38%.

[n-Bu$_2$SnCl$_2$(dmtp)] (**5**): di-n-butyltin dichloride (2 mmol) and dmtp (2 mmol) were mixed in diethyl ether (20 mL); the resulting clear solution was stirred at room temperature for 24 h, then evaporated to dryness under vacuum. m.p. 69–70 °C. Anal. Calc. for C$_{15}$H$_{26}$Cl$_2$N$_4$Sn (452.02 g mol^{-1}): C, 39.86; H, 5.80; N, 12.40; Cl, 15.69. Found: C, 40.10; H, 5.94; N, 12.30; Cl, 16.04%.

[Ph$_2$SnCl$_2$(dmtp)] (**6**): diphenyltin dichloride (2 mmol) and dmtp (2 mmol) were mixed in diethyl ether (20 mL); the resulting clear solution was stirred at room temperature for two days: a white precipitate separated, which was collected and dried under vacuum. m.p. 112–114 °C. Anal. Calc. for C$_{19}$H$_{18}$Cl$_2$N$_4$Sn (492.00 g mol^{-1}): C, 46.39; H, 3.69; N, 11.39; Cl, 14.41. Found: C, 46.45; H, 3.49; N, 11.65; Cl, 14.24%.

2.3. Quantum chemical calculations

DFT calculations, with full optimization of the geometry, were performed by the hybrid B3LYP method and using the double-zeta valence plus polarization (DZVP) all electron basis set [7], on the ligand [1,2,4]triazolo-[1,5-a]pyrimidine (tp), as well as on the two isomeric complexes R$_2$SnCl$_2$(tp)$_2$, R = Me and Et, shown in Fig. 3, by using the GAUSSIAN98 [8] program package. The structures of the two isomers selected were corresponding to the lowest

energy minima found, after a preliminary conformational analysis at the same level of theory, on the five different trial structures deriving from *cis* or *trans* disposition of the Cl$_2$, R$_2$ and (tp)$_2$ ligands. Geometrical parameters and relative energy values are reported in Table 3.

The ^{119}Sn Mössbauer nuclear quadrupole splitting (ΔE) of the organotin(IV) complexes (Table 3) was calculated as recently reported [9], by the calibration formula $\Delta E_{calcd} = 0.93V \pm 0.58$ mm s^{-1}, where $V = V_{zz}[1 + \frac{1}{3} \times (\frac{V_{xx} - V_{yy}}{V_{zz}})^2]^{1/2}$ and where V_{xx}, V_{yy}, V_{zz}, following the condition $|V_{zz}| \geqslant |V_{yy}| \geqslant |V_{xx}|$, are the eigenvalues of the diagonalized electric field gradient tensor, obtained at the same level of theory [9].

2.4. Antimicrobial activity

2.4.1. Microorganisms

The microbial strains used were *E. coli* ATCC 25922, *P. aeruginosa* ATCC 9027, *S. aureus* ATCC 25923, *Staphylococcus epidermidis* DSM 3269, *C. albicans* ATCC 10231 and *C. tropicalis* ATCC 13803.

2.4.2. Antibacterial activity

The determination of the minimum inhibitory concentration (MIC) by broth dilution micro-method was performed as reported [3]. For comparative purposes and quality control of the method, we tested the antibiotic amikacin.

2.4.3. Biofilms susceptibility testing, methylthiazotetrazolium (MTT) method

The tests were performed as previously reported [3] on *S. aureus* ATCC 25923 [10] biofilms employing drug

Table 3
Geometrical parameters (bond distances, in Å, and angles, in degrees), their relative energy and calculated nuclear quadrupole splitting values [8], calculated at DFT level (see text) for the compounds shown in Fig. 3

	tp	Me$_2$SnCl$_2$(tp)$_2$	Me$_2$SnCl$_2$(tp)$_2$	Et$_2$SnCl$_2$(tp)$_2$	Et$_2$SnCl$_2$(tp)$_2$
		A	B	A	B
Sn–N(3)	–	3.008	2.470	2.992	2.423
Sn–N(3′)	–	3.028	2.470	3.120	2.605
Sn–C	–	2.157	2.179	2.179	2.201
Sn–C′	–	2.161	2.166	2.182	2.190
Sn–Cl	–	2.452	2.548	2.452	2.553
Sn–Cl′	–	2.440	2.630	2.450	2.645
N(1)–C(2)	1.340	1.336	1.330	1.337	1.331
C(2)–N(3)	1.353	1.356	1.360	1.356	1.360
N(3)–C(3)	1.335	1.337	1.343	1.338	1.342
C(3)–N(8)	1.405	1.399	1.393	1.399	1.393
C(3)–N(4)	1.348	1.345	1.340	1.345	1.340
N(4)–C(5)	1.322	1.323	1.323	1.322	1.323
C(5)–C(6)	1.425	1.423	1.423	1.423	1.423
C(6)–C(7)	1.374	1.374	1.374	1.374	1.374
C(7)–N(8)	1.357	1.357	1.358	1.357	1.358
N(1)–N(8)	1.358	1.359	1.363	1.359	1.363
C–Sn–C′	–	135.5	179.5	136.4	171.1
N(3)–Sn–N(3′)	–	106.1	168.6	103.5	167.4
Cl–Sn–Cl′	–	97.2	176.6	97.4	168.3
N(3)–Sn–Cl	–	78.7	95.5	78.8	87.2
N(3)–Sn–Cl′	–	175.4	84.4	175.5	81.5
N(3′)–Sn–Cl	–	175.2	95.6	177.6	105.5
N(3′)–Sn–Cl′	–	78.1	84.4	80.2	85.9
N(1)–C(2)–N(3)	117.1	116.6	115.7	116.6	115.7
C(2)–N(3)–C(3)	103.0	103.2	104.2	103.2	104.1
N(3)–C(3)–N(8)	108.5	108.3	107.4	108.3	107.5
C(3)–N(4)–C(5)	116.4	116.3	116.1	116.3	116.1
N(4)–C(5)–C(6)	124.4	124.3	124.2	124.2	124.2
C(5)–C(6)–C(7)	118.6	118.6	118.6	118.6	118.6
C(6)–C(7)–N(8)	116.9	116.9	116.9	116.9	116.9
C(7)–N(8)–C(3)	122.1	122.0	121.7	122.0	121.7
Energy (kJ/mol)	–	0.0	21.3	0.0	22.4
ΔE_{calcd} (mm s^{-1})	–	2.82	4.15	2.89	4.10

concentrations, in Mueller–Hinton broth, ranging from 100 to 6.2 μg/mL, the MIC of n-Bu$_2$SnCl$_2$(dmtp) (**5**).

2.4.4. Biofilms susceptibility testing, crystal violet method

S. aureus ATCC 25923 was cultivated, diluted and the wells were washed as for the MTT method. The plates were air dried at 37 °C and to each well, 100 μL of Mueller–Hinton broth, supplemented with the same concentration of n-Bu$_2$SnCl$_2$(dmtp) used for MTT method, were added. The plates were incubated at 37 °C for 24 h; after this incubation time the medium was removed, the plates were air dried and each well was filled with crystal violet solution (0.1%) for 15–20 min. After this time the plate was washed three times with water and the crystal violet was dissolved adding 150–200 μL of ethanol. The plate was read at 570 nm using a microplate reader. Inhibition percentages at several concentrations of n-Bu$_2$SnCl$_2$(dmtp) were obtained by comparing the optical density of control wells with that of sample wells.

2.4.5. Antifungal activity

The determination of MICs by broth dilution was effected as previously reported [3].

Amphotericin B was used for comparative purpose and quality control of the method.

Biological activity data are reported in Table 6 and in Fig. 4.

3. Results and discussion

3.1. Solid state structures of the adducts

Me$_2$SnCl$_2$ and Et$_2$SnCl$_2$ react with tp and dmtp in diethyl ether to give addition compounds with 1:2 organotin(IV):ligand stoichiometry, while 1:1 adducts were obtained by reaction of n-Bu$_2$SnCl$_2$ and Ph$_2$SnCl$_2$ with dmtp.

Monodentate binding through the endocyclic nitrogen atom N(3) (see Fig. 1) is recognized as the main coordination behaviour of tp and dmtp [1]. It has been observed that the coordination of metal ions through N(3) results in a shift of v_{tp} and v_{py} bands, assigned to triazolopyrimidine and pyrimidine ring mode vibrations, respectively, usually towards higher frequencies [11–18]. The shifts observed in the spectra of our complexes, reported in Table 1, are consistent with N(3) coordination of the organotin(IV)

moiety. The 1:2 complexes $Me_2SnCl_2(tp)_2$, Me_2SnCl_2-$(dmtp)_2$ and $Et_2SnCl_2(dmtp)_2$ show high ^{119}Sn Mössbauer quadrupole splitting values, characteristic of octahedral *trans*-R_2 structures, while the ΔE value observed for $Et_2SnCl_2(tp)_2$ points out that this compound assumes a lower symmetry structure (see Table 2). In the infrared spectra of $Me_2SnCl_2(tp)_2$, $Me_2SnCl_2(dmtp)_2$ and Et_2SnCl_2-$(dmtp)_2$ only one v(Sn–Cl) absorption is observed, at 255, 259 and 231 cm^{-1}, respectively, indicative of a *trans*-Cl_2 arrangement. The resulting all-*trans* configuration (structure I in Fig. 2) is generally adopted by octahedral complexes of transition metals with triazolopyrimidine ligands [1]. A medium intensity band at 573 cm^{-1} in the spectrum of $Me_2SnCl_2(dmtp)_2$, can be attributed to the v_{asym}(Sn–C_2); the analogous band expected in the spectrum of $Me_2SnCl_2(tp)_2$ is probably masked by a ligand absorption at the same frequency.

A different structure must be adopted by the diethyl-tin(IV) derivative, $Et_2SnCl_2(tp)_2$. Mössbauer and infrared data clearly indicate that the C–Sn–C fragment is not linear. Following the Parish approach [19], which assumes that the quadrupole splitting of diorganotin(IV) derivatives is set up just by the Alk_2Sn unit, employing the pqs $[Alk]^{oct} = -1.03$ mm s^{-1} [20], a C–Sn–C angle of 141° was estimated. The infrared spectrum shows two weak bands at 533 and 497 cm^{-1} which can be attributed to v_{asym}(Sn–C_2) and v_{sym}(Sn–C_2) respectively, as expected for a bent C–Sn–C arrangement. Two strong absorptions, at 322 and 251 cm^{-1}, are probably associated to stretching vibrations v(Sn–Cl). These data are consistent with a
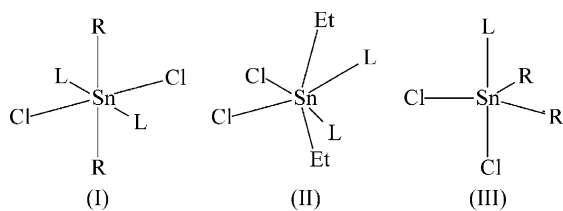

Fig. 2. Proposed structures for R_2SnL_2 and R_2SnL complexes: (I) R = Me; L = tp, dmtp; R = Et; L = dmtp. (II) L = tp. (III) R = *n*-Bu, Ph; L = dmtp.

"skew-trapezoidal" structure, which can be regarded as a distorted *cis*-Cl_2, *cis*-N(3)$_2$, *trans*-R_2 octahedral structure with Sn–C bonds pointing between the couple of ligands with the largest L–Sn–L angle (structure II in Fig. 2).

To rationalize these structural differences, DFT calculations were performed on $R_2SnCl_2(tp)_2$ compounds (R = Me, Et), and the two lowest energy structures found, i.e., the *trans*-R_2 isomers with *cis*-Cl_2 and *trans*-Cl_2, are shown in Fig. 3A and B, respectively. Their relevant geometrical parameters, relative energy and calculated ΔE values are reported in Table 3.

The results obtained point out that the structure of the *cis*-Cl_2 isomer, in vacuo, is more than 20 kJ/mol (see Table 3) more stable than the one corresponding to the *trans*-Cl_2 isomer, for both $Me_2SnCl_2(tp)_2$ and $Et_2SnCl_2(tp)_2$ compounds. On the other hand, the comparison of the calculated and experimental nuclear quadrupole splitting values (Tables 2 and 3) would indicate that the preferred geometry is $Me_2SnCl_2(tp)_2$_B, i.e., the all-*trans* geometry,
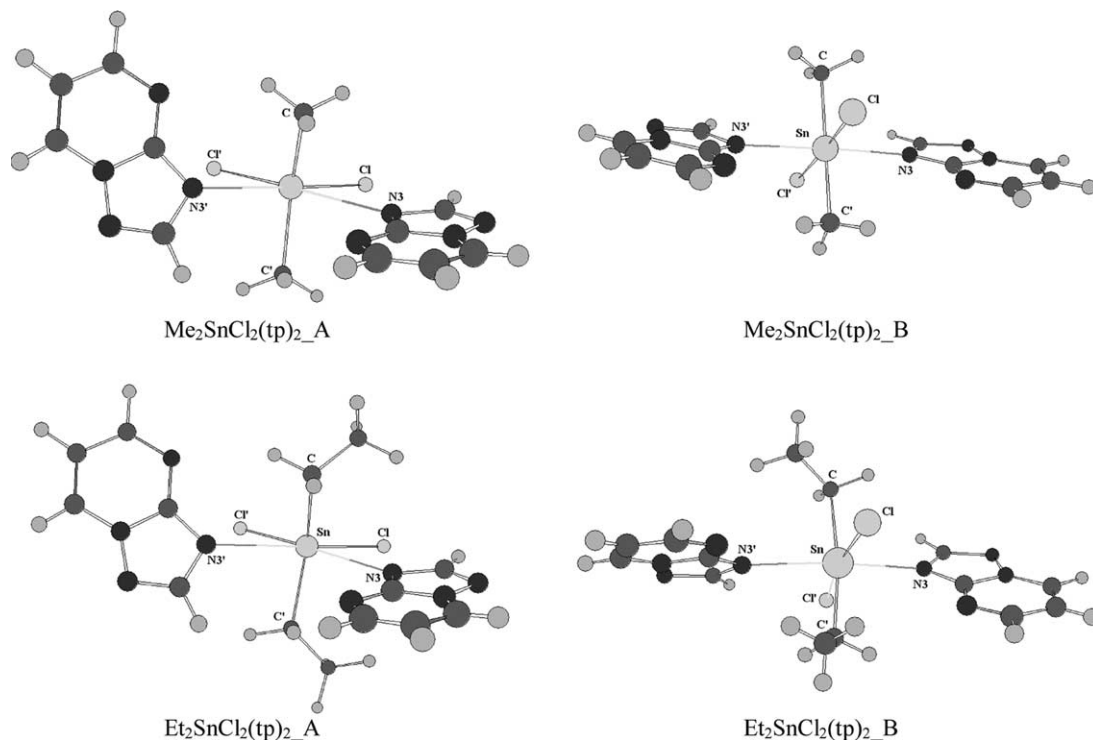

Fig. 3. Calculated structures of two possible R_2SnCl_2 adducts with two tp ligands (R = Me, Et), obtained after full geometry optimization at DFT level (see text). The structures considered present a *trans*-dialkyl geometry, with a *cis*-Cl_2 (A) or *trans*-Cl_2 (B) coordination.

and Et$_2$SnCl$_2$(tp)$_2$_A, i.e., the *trans*-diethyl, *cis*-Cl$_2$ geometry, (see also Fig. 2 for their schematic representation).

In fact, concerning the structure of the compound Et$_2$SnCl$_2$(tp)$_2$, there is a better agreement between the experimental ΔE, 3.45 mm s^{-1} (see Table 2) and the calculated value relative to the most stable structure, Et$_2$SnCl$_2$(tp)$_2$_A, 2.89 mm s^{-1}, compared to that calculated for Et$_2$SnCl$_2$(tp)$_2$_B, 4.10 mm s^{-1} (see Table 3). It is noteworthy the good agreement between the calculated value of the C–Sn–C angle of Et$_2$SnCl$_2$(tp)$_2$_A, 136.4° (Table 3), and the one evaluated by the point charge formalism, 141°, for the same structural environment (see above).

Concerning the structure of the compound Me$_2$Sn-Cl$_2$(tp)$_2$, on the other hand, the preferred structure would not be the most energetically stable in vacuo, i.e., Me$_2$SnCl$_2$(tp)$_2$A, because a much better agreement between the experimental and calculated ΔE is found for Me$_2$SnCl$_2$(tp)$_2$_B, i.e., 4.16 and 4.15 mm s^{-1}, respectively (see Tables 2 and 3).

The preference for the all-*trans* structure can be rationalized in terms of self-assembly through π–π stacking. In fact, we may hypothesize that strong π–π stacking interactions are present in the solid phase among the Me$_2$SnCl$_2$(tp)$_2$ species, through the planar ligands. Analogous interactions have been observed also for metal complexes with similar ligands [21,22]. This intermolecular interaction should be favoured by the almost coplanar disposition of the two coordinated tp ligands, as observed in Me$_2$SnCl$_2$(tp)$_2$_B, compared to the almost perpendicular disposition of the two planar ligands in Me$_2$SnCl$_2$(tp)$_2$_A.

On the other hand, the almost perpendicular disposition of the two planar ligands in Et$_2$SnCl$_2$(tp)$_2$_A (see Fig. 3) would hinder the self-assembly process through π–π stacks.

Our hypothesis is supported by the circumstance that Me$_2$SnCl$_2$(tp)$_2$ exhibits Mössbauer spectrum at room temperature (see Table 2) characterized by a relatively large area, compared to that of the liquid-nitrogen temperature spectrum. Assuming a linear trend of the function $\ln(A)$ vs. T, a value of ca. 0.01 is found for $d\ln(A)/dT$, wich is typical of polymeric R$_2$Sn(IV) compounds [23]. On the other hand, no room temperature ^{119}Sn Mössbauer effect was occurring for Et$_2$SnCl$_2$(tp)$_2$.

The Mössbauer spectra of the dimethyl and diethyltin(IV) adducts of dmtp, compounds **3** and **4**, are characterized by quadrupole splitting values which are very close to that of Me$_2$SnCl$_2$(tp)$_2$; on this base, we can hypothesize they have the same structure, probably stabilized by π–π stacking, also considering that the presence of the methyl groups in positions 5 and 7 (see Fig. 1) would favour the stacking interactions by electron releasing effects on the aromatic system of the ligand.

As already mentioned, *n*-Bu$_2$SnCl$_2$ and Ph$_2$SnCl$_2$, probably due to the bulkiness of the organic groups, give 1:1 addition compounds with dmtp. As a consequence, excluding a polydentate coordination, tin is presumably five-coordinated. Assuming a trigonal bipyramidal configuration, the presence of two ν(Sn–Cl) absorptions is indicative of a *cis*-Cl$_2$ configuration in both the complexes. It is not possible to assign Sn–C vibrations, because these are masked by the ligand's absorption bands. On the other hand, it is well-known that, according to the Bent rule [24], organic groups bound to tin normally occupy equatorial positions. Accordingly, the complexes should have the structure III in Fig. 2, with the organic groups and a chlorine atom in the equatorial plane while a chlorine atom and the dmtp molecule occupy the axial positions.

The ^{119}Sn Mössbauer parameters are consistent with the proposed structure: the C–Sn–C angle estimated by the Parish approach [19] is 126° for *n*-Bu$_2$SnCl$_2$ (dmtp) ([Alk]^{tbe} = −1.13 mm s^{-1} [25]) and 129° for Ph$_2$SnCl$_2$(dmtp) ([Ph]^{tbe} = −0.98 mm s^{-1} [25]). Point-charge model calculations [26] do not allow us to definitely establish if the ligand occupy an axial (*cis*-Cl$_2$ configuration) or equatorial (*trans*-Cl$_2$ configuration) position, as the contributions of nitrogen and chlorine atoms to the electrical field gradient on ^{119}Sn nucleus are quite similar. However, the presence of two ν(Sn–Cl) absorptions allows us to exclude the *trans*-Cl$_2$ configuration.

3.2. Methanol solution studies

The adducts were tested for their in vitro antimicrobial activity; the nature of the complexes in solution phase was investigated by means of ^{1}H and ^{13}C NMR (Tables 4 and 5)

Table 4
^{1}H NMR spectra of tp and dmtp and their diorganotin(IV) chloride adducts[a]

		H-2	H-5	H-6	H-7	CH$_3$	R–Sn	$\|^2J(^1\text{H}-^{119}\text{Sn})\|$
	tp	8.58	8.91	7.35	9.23			
1	Me$_2$SnCl$_2$(tp)$_2$	8.58	8.91	7.35	9.23		1.11	94.7
	Me$_2$SnCl$_2$[b]	–	–	–	–		1.21	94.0
							1.18	94.6
2	Et$_2$SnCl$_2$(tp)$_2$	8.58	8.91	7.36	9.23			
	dmtp	8.47	–	7.12	–	2.65, 2.81		
3	Me$_2$SnCl$_2$(dmtp)$_2$	8.47	–	7.13	–	2.65, 2.81	1.12	94.4
4	Et$_2$SnCl$_2$(dmtp)$_2$	8.47	–	7.12	–	2.65, 2.81		
5	Bu$_2$SnCl$_2$(dmtp)[b]	8.47	–	7.13	–	2.65, 2.81	0.92–1.81	
6	Ph$_2$SnCl$_2$(dmtp)	8.48	–	7.12	–	2.66, 2.80	7.40–8.06	

[a] In CD$_3$OD; δ in ppm from internal TMS; coupling constants in MHz.
[b] Ref. [31].

Table 5
^{13}C NMR spectra of the complexes **2**–**6** and related compounds[a]

		C-2	C-3a	C-5	C-6	C-7	CH$_3$	R–Sn	
	tp	157.17	155.92	156.5	112.40	138.54	–		
2	Et$_2$SnCl$_2$(tp)$_2$	157.14	156.09	156.37	112.42	138.48	–	25.01(α), 10.23(β)	^1J(Sn–C) = 682.7 ^2J(Sn–C) = 50.7
	dmtp	155.62	156.01	167.37	112.48	149.30	16.81, 24.74		
4	Et$_2$SnCl$_2$(dmtp)$_2$	155.42	155.91	167.29	112.44	149.19	16.76, 24.70	24.79(α), 10.16(β)	^1J(Sn–C) = 683.1 ^2J(Sn–C) = 50.7
5	Bu$_2$SnCl$_2$(dmtp)	155.35	155.80	167.39	112.59	149.23	16.87, 24.82	30.98(α), 28.40(β), 27.05(γ), 13.93(δ)	^1J(Sn–C) = 619.5 ^2J(Sn–C) = 40.9 ^3J(Sn–C) = 111.3
	Bu$_2$SnCl$_2$	–	–	–	–	–	–	30.87(α), 28.42(β), 27.09(γ), 13.94(δ)	^1J(Sn–C) = 619.6 ^2J(Sn–C) = 40.9 ^3J(Sn–C) = 111.9
6	Ph$_2$SnCl$_2$(dmtp)	154.96	155.50	167.58	112.74	149.26	16.84, 24.81	145.11(*ipso*), 136.14(*ortho*), 129.71(*meta*), 131.07(*para*)	^2J(Sn–C) = 65.4 ^3J(Sn–C) = 100.7 ^4J(Sn–C) = 19.9

[a] In CD$_3$OD; δ in ppm from internal TMS; ^nJ(Sn–C) = $|^nJ(^{119}$Sn–^{13}C)|, MHz.

and ^{119}Sn Mössbauer (Table 2) spectroscopy in CD$_3$OD and CH$_3$OH, respectively. Both techniques would suggest that the adducts dissociate in methanol. In fact, the ^{1}H and ^{13}C chemical shifts of the ligand atoms in CD$_3$OD are practically identical for the complexes and the free ligands, the differences being within the limits of the measurement error. It is, however, worth mentioning that the lack of any shift in ^{1}H and ^{13}C ligand signals was already observed in stable metal complexes of dmtp and analogous ligands [11].

Information on the tin environment was deduced from $|^2J(^{119}$Sn–^{1}H)$|$ and $|^1J(^{119}$Sn–^{13}C)$|$ coupling constants, such as from ^{119}Sn Mössbauer quadrupole splitting values measured in frozen solutions, which correlate with the C–Sn–C bond angles [27,19]. The quadrupole splittings (Table 2) and the coupling constants (Tables 4 and 5) measured for the complexes are very similar to those of the parent diorganotin(IV) chlorides; ^{119}Sn Mössbauer data suggest *trans*-R$_2$ octahedral structures for the diorganotin(IV) moieties while ^{13}C NMR data relative to **2**, **4** and **5** are compatible with lower coordination numbers or symmetry being the calculated [27] C–Sn–C bond angle 137° for **2** and **4** and 131° for **5**. These differences may be related to the freezing process needed for the Mössbauer measurements which may be associated to crystallization processes. Anyhow, the close similarity of the parameters relative to the organotins and to the complexes does not support the hypothesis of interaction, in solution, between the organotin(IV) dichlorides and tp and dmtp molecules.

The correspondence of the spectroscopic signals of the complexes with those of the parent ligands and organotin moieties, would explain the observed biological activity of compounds **1**–**4**, (see below). However, the analogous results obtained for compounds **5** and **6** do not agree with the interesting antimicrobial properties for compounds **5** and, to a lesser extent, **6** (see Section 3.3), for which some cooperative effect is developed in such systems, in contrast with the apparent dissociation of the complexes in solution.

An accurate further characterization of the solution phases of **5** and **6**, e.g., by potentiometric titrations, seems to be necessary to explain their biological effects.

3.3. Antimicrobial activity

3.3.1. MIC, anti-biofilm and antifungal results
The compounds were screened for their in vitro antimicrobial activity on a group of representative Gram-positive, Gram-negative bacteria and two human pathogen fungal strains.

The antimicrobial activities of substances, expressed as MIC are reported in Table 6.

The ligands tp and dmtp resulted inactive at screening concentration of 100 µg/mL, but their complexation with organotin led to derivatives with a better antimicrobial activity. However, the activity of the complexes did not always result better than that of the parent organotin compounds. In particular, Et$_2$SnCl$_2$ and its derivatives Et$_2$SnCl$_2$(tp)$_2$ and Et$_2$SnCl$_2$(dmtp)$_2$ showed about the same activity against Gram negative *E. coli*, *P. aeruginosa* and Gram positive *S. aureus* with MIC values ranging from 25 to 50 µg/mL and none of them resulted active against *S. epidermidis*. Concerning *n*-Bu$_2$SnCl$_2$(dmtp), we observed an improvement of activity against *E. coli* and *S. aureus* with MIC value of 6.2 µg/mL in both cases. A good activity (MIC equal to 3.1 µg/mL) against *S. epidermidis* is exhibited by Ph$_2$SnCl$_2$(dmtp).

Most compounds resulted inactive as antifungal at screening concentration of 100 µg/mL or showed a weak activity, in fact the MIC values ranged from 25 to 100 µg/mL (see Table 6).

Considering the important role played by staphylococci in biofilm-associated infections [28], we also decided to test the derivative *n*-Bu$_2$SnCl$_2$(dmtp) (**5**), which showed a good activity on *S. aureus*, against preformed biofilms of the same strain. We obtained inhibition percentages ranging

Table 6
Antimicrobial activity in vitro, MIC values in µg/mL

Compound	*E. coli* ATCC 25922	*P. aeruginosa* ATCC 9027	*S. aureus* ATCC 25923	*S. epidermidis* DSM 3269	*C. albicans* ATCC 10231	*C. tropicalis* ATCC 13803
Me$_2$SnCl$_2$	>100	100	100	>100	>100	>100
Me$_2$SnCl$_2$(tp)$_2$	>100	>100	>100	>100	>100	>100
Me$_2$SnCl$_2$(dmtp)$_2$	>100	>100	>100	>100	>100	>100
Et$_2$SnCl$_2$	25	25	25	>100	>100	>100
Et$_2$SnCl$_2$(tp)$_2$	25	25	50	>100	>100	>100
Et$_2$SnCl$_2$(dmtp)$_2$	50	50	50	>100	>100	>100
Bu$_2$SnCl$_2$	100	>100	50	6.2	100	100
Bu$_2$SnCl$_2$(dmtp)	6.2	>100	6.2	6.2	>100	>100
Ph$_2$SnCl$_2$	50	>100	25	25	50	50
Ph$_2$SnCl$_2$(dmtp)	100	>100	25	3.1	50	25
tp	>100	>100	>100	>100	>100	>100
dmtp	>100	>100	>100	>100	>100	>100
Amikacin	10	5	1	0.62	–	–
Amphotericin B	–	–	–	–	0.15	0.31

from 76.3% to 17.2% or 45.5% to 16.1% at concentrations ranging from 100 to 6.2 µg/mL (Fig. 4) using, respectively, MTT or crystal violet method for staining biofilms grown in microtiter plates.

This discrepancy in the observed data, with reference to the method used to staining biofilms, is due to the different information derived from these methods; in fact MTT is a respiratory indicator and in this way we can detect killing activity of **5**, whereas crystal-violet staining, as an indicator of total attached biomass, shows removing activity of compound. Compound **5** has a better killing effect on the staphylococcal biofilm rather than removing the biofilm itself.

Biofilms of staphylococci represent an intrinsic form of resistance to antibiotics, they are causes of colonization on the surface of important indwelling medical devices (catheters and other plastic foreign bodies) and are difficult to treat and persistent infections. Antibiofilm activity should then be considered an important factor in evaluating compounds as candidates for further development stages in antimicrobial research [29]; for this reason we think that **5** might be a potential lead compound in the discovery of new anti Gram-positive and antibiofilm agents.

Fig. 4. In vitro inhibition percentages on *S. aureus* ATCC 25923 biofilm obtained for *n*-Bu$_2$SnCl$_2$(dmtp) with MTT and crystal-violet methods. Values are the average of at least three independent determinations. The coefficient of variation was less than 15%.

References

[1] J.M. Salas, M.A. Romero, M.P. Sánchez, M. Quirós, Coord. Chem. Rev. 193–195 (1999) 1119.
[2] J.G. Haasnot, Coord. Chem. Rev. 200–202 (2000) 131.
[3] M.A. Girasolo, C. Di Salvo, D. Schillaci, G. Barone, A. Silvestri, G. Ruisi, J. Organomet. Chem. 690 (2005) 4773.
[4] J.M. Salas, A. Rahmani, M.A. Romero, A.D. Rae, A.C. Willis, E.R.T. Tiekink, Z. Kristallogr. 213 (1998) 302.
[5] W. Schöniger, Mikrochim. Acta (1955) 123.
[6] A. Barbieri, G. Ruisi, A. Silvestri, A.M. Giuliani, A. Barbieri, G. Spina, F. Pieralli, F. Del Giallo, J. Chem. Soc., Dalton Trans. (1995) 467, and refs. therein.
[7] (a) N. Godbout, D.R. Salahub, J. Andzelm, E. Wimmer, Can. J. Chem. 70 (1992) 560;
(b) C. Sosa, J. Andzelm, B.C. Elkin, E. Wimmer, K.D. Dobbs, D.A. Dixon, J. Phys. Chem. 96 (1992) 6630.
[8] M.J. Frisch, G.W. Trucks, H.B. Schlegel, G.E. Scuseria, M.A. Robb, J.R. Cheeseman, V.G. Zakrzewski, J.A. Montgomery Jr., R.E. Stratmann, J.C. Burant, S. Dapprich, J.M. Millam, A.D. Daniels, K.N. Kudin, M.C. Strain, O. Farkas, J. Tomasi, V. Barone, M. Cossi, R. Cammi, B. Mennucci, C. Pomelli, C. Adamo, S. Clifford, J. Ochterski, G.A. Petersson, P.Y. Ayala, Q. Cui, K. Morokuma, D.K. Malick, A.D. Rabuck, K. Raghavachari, J.B. Foresman, J. Cioslowski, J.V. Ortiz, A.G. Baboul, B.B. Stefanov, G. Liu, A. Liashenko, P. Piskorz, I. Komaromi, R. Gomperts, R.L. Martin, D.J. Fox, T. Keith, M.A. Al-Laham, C.Y. Peng, A. Nanayakkara, M. Challacombe, P.M.W. Gill, B. Johnson, W. Chen, M.W. Wong, J.L. Andres, C. Gonzalez, M. Head-Gordon, E.S. Replogle, J.A.
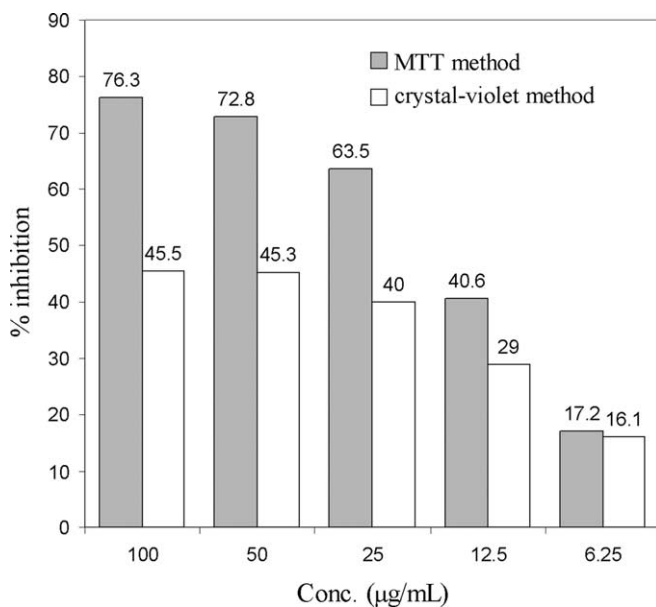
Pople, GAUSSIAN98, Revision A.8, Gaussian, Inc., Pittsburgh, PA, 1998.

[9] G. Barone, A. Silvestri, G. Ruisi, G. La Manna, Chem. Eur. J. 11 (2005) 6185.

[10] C. Heilmann, C. Gerke, F. Pendreau-Remington, F. Götz, Infect. Immun. 64 (1996) 277.

[11] E. Szłik, A. Grodzicki, L. Pazderski, J. Sitkowski, Polish J. Chem. 72 (1998) 55.

[12] I. Łakomska, E. Szłyk, J. Sitkowski, L. Kozerski, J. Wietrzyk, M. Pełczynska, A. Nasulewicz, A. Opolski, J. Inorg. Biochem. 98 (2004) 167.

[13] E. Szłyk, L. Pazderski, I. Łakomska, A. Surdykowski, T. Glowiak, J. Sitkowski, L. Kozerski, Polyhedron 21 (2002) 343.

[14] E. Szłyk, A. Grodzicki, L. Pazderski, E. Bednarek, B. Kamienski, Polyhedron 19 (2000) 965.

[15] E. Szłyk, I. Łakomska, A. Surdykowski, T. Glowiak, L. Pazderski, J. Sitkowski, L. Kozerski, Inorg. Chim. Acta 333 (2002) 93.

[16] J.M. Salas, M.A. Romero, A. Rahmani, R. Faure, G. Alvarez de Cienfuegos, E.R.T. Tiekink, J. Inorg. Biochem. 64 (1996) 259.

[17] E. Szłik, A. Grodzicki, L. Pazderski, A. Wojtczak, J. Chatłas, G. Wrzeszcz, J. Sitkowski, B. Kamieński, J. Chem. Soc., Dalton Trans. (1998) 901.

[18] A.H. Velders, L. Pazderski, F. Ugozzoli, M. Biagini-Cingi, A.M. Manotti-Lanfredi, J.G. Haasnot, J. Reedijk, Inorg. Chim. Acta 273 (1998) 259.

[19] R.V. Parish, Structure and bonding in tin compounds, in: G.J. Long (Ed.), Mössbauer Spectroscopy Applied to Inorganic Chemistry, Plenum Press, New York, 1984, pp. 527–575 (Chapter 16).

[20] M.G. Clark, A.G. Maddock, R.H. Platt, J. Chem. Soc., Dalton Trans. (1972) 281.

[21] S. Orihuela, M.P. Sánchez, M. Quirós, J. Molina, R. Faure, J. Mol. Struct. 415 (1997) 285.

[22] J.M. Salas, J.A.R. Navarro, M.A. Romero, M. Quirós, An. Quim. Int. Ed. 93 (1997) 55.

[23] R. Barbieri, F. Huber, L. Pellerito, G. Ruisi, A. Silvestri, Tin-119m Mössbauer Studies on Tin Compounds, in: P.J. Smith (Ed.), Chemistry of Tin, Chapman and Hall, London, 1998, p. 496 (Chapter 14).

[24] H.A. Bent, Chem. Rev. 61 (1961) 275.

[25] G.M. Bancroft, V.G. Kumar Das, T.K. Sham, M.G. Clark, J. Chem. Soc., Dalton Trans. (1976) 643.

[26] G.M. Bancroft, R.H. Platt, Adv. Inorg. Chem. Radiochem. 15 (1972) 59.

[27] T.P. Lockart, W.F. Manders, J.J. Zuckerman, J. Am. Chem. Soc. 107 (1985) 4546.

[28] F. Götz, Mol. Microbiol. 43 (2002) 1367.

[29] S.J. Projan, P.J. Youngman, Curr. Opin. Microbiol. 5 (2002) 463.

[30] R.C. Poller, J. Nucl. Chem. 24 (1962) 593.

[31] F. Caruso, M. Giomini, A.M. Giuliani, E. Rivarola, J. Organomet. Chem. 506 (1996) 67.